CHIN. PHYS. LETT. Vol. 38, No. 6 (2021) 060302

Topological Knots in Quantum Spin Systems

X. M. Yang(杨学敏), L. Jin(金亮)*, and Z. Song(宋智)*

School of Physics, Nankai University, Tianjin 300071, China

(Received 26 February 2021; accepted 19 April 2021; published online 25 May 2021)

Knot theory provides a powerful tool for understanding topological matters in biology, chemistry, and physics. Here knot theory is introduced to describe topological phases in a quantum spin system. Exactly solvable models with long-range interactions are investigated, and Majorana modes of the quantum spin system are mapped into different knots and links. The topological properties of ground states of the spin system are visualized and characterized using crossing and linking numbers, which capture the geometric topologies of knots and links. The interactivity of energy bands is highlighted. In gapped phases, eigenstate curves are tangled and braided around each other, forming links. In gapless phases, the tangled eigenstate curves may form knots. Our findings provide an alternative understanding of phases in the quantum spin system, and provide insights into one-dimension topological phases of matter.

DOI: 10.1088/0256-307X/38/6/060302

Knots are categorized in terms of geometric topology, and describe topological properties of one-dimensional (1D) closed curves in a three-dimensional space.[1,2] A collection of knots without an intersection forms a link. The significance of knots in science is elusive. However, knot theory can be used to characterize topologies of DNA structures[3] and synthesized molecular structures[4] in biology and chemistry. Knot theory is used to solve fundamental questions in physics ranging from microscopic to cosmic textures and from classical mechanics to quantum physics.[5−12] Knots and links are observed for vortices in fluids,[13−15] lights,[16,17] and quantum eigenfunctions,[18] for solitons in Bose–Einstein condensates,[19] and for Fermi surfaces of topological semimetals in Hermitian[20−32] and non-Hermitian systems.[33−39] Knots and links with distinctive geometric topological features are crucial for understanding hidden physics.

Innovations in visualization have driven scientific developments. Historically, Feynman diagrams are created to provide a convenient approach for describing and calculating complex physical processes in quantum theory.[40] Feynman diagrams help to understand interactions between particles and provide a thorough understanding of the foundations of quantum physics. In condensed matter physics, a coherent description of matter is difficult because of the complexity of its phases. In 1D topological systems, phases of matter are generally characterized using a winding number associated with a Zak phase (a physical quantity used to characterize the topological property of 1D systems)[41] of the corresponding band. Topological phases with different winding numbers are considerably different from each other, and differences in their topological properties can be attributed to the eigenstates. The winding numbers and Zak phases are defined for separate energy bands. In the gapless phase, the boundaries of different gapped phases should have different topological features. However, the energy band is inseparable. The compatible characterization of gapped and gapless phases is a concern.

In this work, a graphic approach is developed to examine topological properties and phase transitions in a 1D topological system. The ground states of the quantum spin system are mapped into knots and links; the topological invariants constructed from eigenstates are then directly visualized; and topological features are revealed from the geometric topologies of knots and links. In contrast to the conventional description of band topologies, such as the Zak phase and Chern number (a topological invariant for topological phase of matter in condensed matter physics)[42] that can be extracted from a single band, this approach highlights the interactivity between upper and lower bands; thus, information on two bands is necessary for obtaining a complete eigenstate graph. In contrast to map zero-energy surfaces or Fermi surfaces to knots or links to study their topological properties,[20−32] we emphasize that the eigenstate graph extracts topology information from the eigenstates. Several standard processes have been performed to diagonalize the Hamiltonian of the quantum spin system. The spin-1/2 spin model is transformed into a spinless fermion under the Jordan–Wigner transformation. In Majorana representation, the core matrix of the spinless fermion

Supported by the National Natural Science Foundation of China (Grants Nos. 11874225, 11975128, and 11605094).
*Corresponding authors. Email: jinliang@nankai.edu.cn; songtc@nankai.edu.cn
© 2021 Chinese Physical Society and IOP Publishing Ltd

system is obtained under Nambu representation. The eigenstates of the core matrix are then mapped into closed curves of knots and links. The graphs of different categories represent different topological phases.

Recently, rich quantum phases,[43–45] exotic Majorana physics[46] and phase transitions[47,48] have been discovered in topological materials. In this work, an exactly solvable generalized XY model with long-range interactions is revisited, which ensures the richness of topological phases.[49] The closed curves of eigenstates completely encode the information on ground states. In topologically nontrivial phases, eigenstate curves are tangled to form links for the gapped phase; however, they may be untied and combined into knots for the gapless phase. Knot theory is developed to characterize the topological features of both gapped and gapless phases. In knot theory,[1] a link is a collection of knots with no intersecting points and a knot can be described as a link with one component. Both links and knots are studied in knot theory. In this approach, the gapped and gapless phases are visualized, and their topological features are revealed through knots and links.

Quantum Spin Model. A solvable generalized 1D XY model with long-range three-spin interactions is considered for elucidation.[50,51] The Hamiltonian is

$$H=\sum_{j=1}^{N}\Big\{\sum_{n=1}^{M}\big(J_n^x\sigma_j^x\sigma_{j+n}^x+J_n^y\sigma_j^y\sigma_{j+n}^y\big)\prod_{l=j+1}^{j+n-1}\sigma_l^z + g\sigma_j^z\Big\}, \tag{1}$$

where operators $\sigma_j^{x,y,z}$ are Pauli matrices for spin at the jth site and the model has periodic boundary conditions. H is reduced to an ordinary anisotropic XY model for $M=1$. A conventional Jordan–Wigner transformation $\sigma_j^z=1-2c_j^\dagger c_j$, $\sigma_j^y=i\sigma_j^x\sigma_j^z$, $\sigma_j^x=-\prod_{l<j}(1-2c_l^\dagger c_l)(c_j+c_j^\dagger)$ for spin-1/2 is performed,[52] and the Hamiltonian of a subspace with odd number particles (fermions) can be expressed using a Hamiltonian describing a spinless fermion as follows:

$$H=\sum_{j=1}^{N}\Big[\sum_{n=1}^{M}\big(J_n^+c_j^\dagger c_{j+n}+J_n^-c_j^\dagger c_{j+n}^\dagger+\text{H.c.}\big) + g\big(1-2c_j^\dagger c_j\big)\Big], \tag{2}$$

where $c_j^\dagger$ (c_j) denotes the creation (annihilation) operator of spinless fermion at the jth site and $J_n^\pm=J_n^x\pm J_n^y$. In large N limit ($N\gg M$), H is available for both parities of particle (fermion) numbers, thus representing a p-wave topological superconducting wire using long-range interactions.[53,54] Majorana fermion operators are introduced, $a_j=c_j^\dagger+c_j$, $b_j=-i(c_j^\dagger-c_j)$, the inverse transformation gives $c_j^\dagger=(a_j+ib_j)/2$, $c_j=(a_j-ib_j)/2$. The Majorana representation of the Hamiltonian is

$$H=i\sum_{j=1}^{N}\Big\{\sum_{n=1}^{M}\big(J_n^xb_ja_{j+n}-J_n^ya_jb_{j+n}\big)+ga_jb_j\Big\}. \tag{3}$$

In the Nambu representation of basis $\psi^{\mathrm{T}}=(a_1,ib_1,a_2,ib_2,\ldots)$, $H=\psi^{\mathrm{T}}h\psi$ and h is a $2N\times 2N$ matrix, which is referred to as the core matrix. Applying Fourier transformation $|a,j\rangle=\frac{1}{\sqrt{2N}}\sum_k e^{ikj}|a,k\rangle$ and $|b,j\rangle=\frac{1}{\sqrt{2N}}\sum_k e^{ikj}|b,k\rangle$ on Eq. (3), we obtain $h=\sum_k h_k$ and

$$h_k=B_x(k)\sigma_x+B_y(k)\sigma_y, \tag{4}$$

with

$$\sigma_x=\begin{pmatrix}0&1\\1&0\end{pmatrix},\quad \sigma_y=\begin{pmatrix}0&-i\\i&0\end{pmatrix}.$$

The components of the effective magnetic field are periodic functions of momentum k,

$$B_x(k)=\sum_{n=1}^{M}\frac{1}{4}[J_n^+\cos(nk)-g],$$
$$B_y(k)=\sum_{n=1}^{M}\frac{1}{4}J_n^-\sin(nk), \tag{5}$$

where k is a 1D coordinate since the systems investigated are 1D. After putting the Jordan–Wigner transformation, Majorana transformation and Fourier transformation on the original Hamiltonian, we obtain the core matrix in the form of $h=\sum_k h_k$ and all information on the system is encoded in matrix h_k, because the eigenvalues and eigenvectors can be employed to construct the complete eigenstates of the original Hamiltonian. A winding number is defined using an effective planar magnetic field (B_x,B_y) as follows:

$$w=\frac{1}{2\pi}\oint_C\frac{1}{B^2}(B_xdB_y-B_ydB_x), \tag{6}$$

where $B=(B_x^2+B_y^2)^{1/2}$, and C is the closed curve of Bloch vector in the B_x–B_y plane; w characterizes a vortex enclosed in the loop. The formation of a vortex depends on whether the Bloch vectors rotate when traversing the Brillouin zone, and w is positive for clockwise rotation, while w is negative for counterclockwise rotation. In the gapped phase, the winding number of the vector field is capable of obtaining from the complex analysis of $B_x(k)+iB_y(k)$ according to Cauchy's argument principle. In the gapless phase, loop C passes through the origin, and integral w depends on the loop path. Although w is crucial for characterizing the gapped phase, w cannot be used to characterize the gapless phase (see the Supplementary Material).

To overcome this concern, a graphic representation is developed to visualize the eigenstates (Fig. 1). The eigenstates in different gapless and gapped phases are

mapped into different categories of torus knots and links. The topological features of the ground state are evident through the geometric topologies of eigenstate knots and links on k–φ tori. Therefore, knot theory in mathematics can characterize topological phases in physics, and different topological phases can be distinguished. In the following sections, we discuss the graphic eigenstate, topological characterization, and knot theory for the topological phases of the quantum spin system.

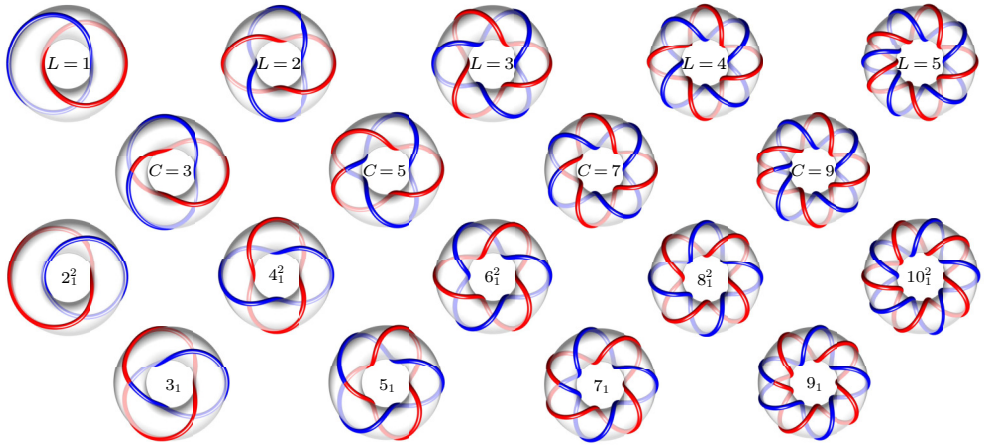

Fig. 1. The upper (lower) two rows are eigenstate knots and links on the k–φ tori with positive (negative) crossing and linking numbers. The first and third rows are the links, the second and fourth rows are the knots. The numbers in the lower two rows indicate the crossing number, and the superscript represents the number of loops, which is absent for the knots. The subscript indicates the order of knot configuration with an identical number of loops and an identical crossing number in the Alexander–Briggs notation.[2] The parameters in Eq. (10) for the 18 knots and links from left to right and from top to bottom are $(x, y) = (1.1, 1.2)$, $(0.5, 1.2)$, $(0, 1.2)$, $(-0.5, 1.2)$, $(-0.8, 1.2)$; $(0.68, 1.2)$, $(0.28, 1.2)$, $(-0.28, 1.2)$, $(-0.68, 1.2)$; $(2, 0.7)$, $(1.8, 0)$, $(1.8, -0.5)$, $(1.8, -1)$, $(1.8, -1.5)$; $(2, 0.21)$, $(1.5, -0.32)$, $(2, -0.75)$, $(2, -1.2)$.

The spectrum of h_k is $\epsilon_k^{\pm} = \pm B$ and the corresponding eigenstate is $|\psi_k^{\pm}\rangle = [e^{i\varphi_{\pm}(k)}, 1]^{\mathrm{T}}/\sqrt{2}$. The phases in eigenstate $|\psi_k^{\pm}\rangle$ are real periodic functions of k, $\varphi_+(k) = \arctan(-B_y/B_x)$, and

$$\varphi_-(k) = \varphi_+(k) + \pi. \tag{7}$$

Accordingly, the ground state of h can be expressed as $|G\rangle = \prod_k |\psi_k^-\rangle$, with ground state energy $E_g = \sum_k \epsilon_k^-$. The ground state phase diagram is obtained using $\epsilon_{k_c}^{\pm} = 0$, where the energy band gap closes.

Knot Topology. The topological features of the ground state are completely encoded in phase factor $\varphi_{\pm}(k)$. In the absence of band degeneracy, the energy bands are gapped and each eigenstate is represented as a closed curve on the surface of an unknotted torus in $\boldsymbol{R}^3$ since $\varphi_{\pm}(k)$ for each particular k only corresponds to a single point in the torus, and the closed curve is formed by traversing the whole Brillouin region. The toroidal direction is k and the poloidal direction is φ (Fig. 1). From $\varphi_-(k) = \varphi_+(k) + \pi$, the two curves are always located at opposite points in the cross section of the torus. For topologically nontrivial phases, they become tangled curves, which are braided around each other. In the presence of band degeneracy, two eigenstates may form one closed curve. The topological properties of the ground state are reflected from the geometric topology of closed curves. The curves on the torus forms a torus knot, which are particular types of knots/links on the surface of an unknotted torus.[1] For the eigenstate graphs of the corresponding quantum spin system, eigenstate graphs are only knots and two-loop links. The rich topological phases of either gapless or gapped, either Hermitian or non-Hermitian band degeneracy, and either trivial or nontrivial phases are all distinguishable from the eigenstate graphs. The graphic approach is employed to distinguish between the real gapless phases arising from exceptional points (the symmetry breaking point of non-Hermitian Hamiltonians, where two or more eigenvalues degenerate and their corresponding eigenvectors coalesce into the same one) and degenerate points (two or more eigenvalues are degenerate and corresponding eigenvectors are still orthogonal to each other), which cannot be distinguished using the two winding numbers in the non-Hermitian system.[37]

For a gapped system, the two loops without any node form a link on the torus. In knot theory, for the topology of the two closed curves (loops) in the three-dimensional space, a linking number is used as a topological invariant.[55] The linking number represents the number of times each curve is braided around the other curve. Mathematically, the linking number of two closed curves $\boldsymbol{r}_+(k)$ and $\boldsymbol{r}_-(k')$ can be calculated using a double line integral:

$$L = \frac{1}{4\pi} \oint_k \oint_{k'} \frac{\boldsymbol{r}_+(k) - \boldsymbol{r}_-(k')}{|\boldsymbol{r}_+(k) - \boldsymbol{r}_-(k')|^3} \cdot [d\boldsymbol{r}_+(k) \times d\boldsymbol{r}_-(k')]. \tag{8}$$

The two curves are the two loops of eigenstates; $|\boldsymbol{r}_+(k) - \boldsymbol{r}_-(k')|$ for $k = k'$ is the cross section diameter of the torus. A straightforward derivation yields (see the Supplementary Material)

$$L = -\frac{1}{2\pi}\int_0^{2\pi} \nabla_k \varphi_+(k) dk, \tag{9}$$

which has a geometrical meaning: the braiding of the two curves on the torus surface. Furthermore, $L = w$ is valid for gapped phases (see the Supplementary Material); and linking number L for the two loops has the same significance as that of winding number w in the characterization of the topology of the ground state.

The gapless phase is the phase transition boundary of different gapped phases.[56] The band degenerate points in a chiral symmetric system have zero energy. In the next few paragraphs, we discuss the formation of gapless knots with an odd number of degenerate points and gapless links with even number of degenerate points. At degenerate points, eigenstates switch and experience a π phase shift in both phase factors $\varphi_\pm(k)$ because $\varphi_+(k)$ and $\varphi_-(k)$ have a phase difference of π (the second and fourth rows in Fig. 1). In the period $[-\pi, \pi]$ of k, the points $k = -\pi$ and $k = +\pi$ are considered as one degenerate point. For the two energy bands with an even number of degenerate points in a 2π period of k, the energy bands are repeated in the subsequent period of k, and the two corresponding separate eigenstate loops are observed. By contrast, for two energy bands with an odd number of degenerate points in a 2π period of k, the two energy bands are switched in the subsequent 2π period of k as they switched odd times because of band degeneracies. In this case, two functions $\varphi_+(k)$ and $\varphi_-(k)$ combine to form a single periodic function and the corresponding eigenstate curves are connected to form a single-loop on the torus. In contrast to a two-loop link, the graph eigenstates comprise a knot.

Alternatively, considering the π phase shift in $\varphi_\pm(k)$ at the band degenerate points, a total phase change is 2π for two eigenstates. When k varies by 2π, in any topological phase with a two-loop link, the accumulation of phase $\varphi_\pm(k)$ is an integer multiple of 2π due to the periodic boundary condition $\varphi_\pm(k) = \varphi_\pm(k + 2\pi) + 2n\pi$ and the total circling $\Phi(k) = \varphi_+(k) + \varphi_-(k)$ is an even times of 2π. Therefore, the appearance of an odd number of degenerate points in the energy band results in the change of an odd times of 2π. Thus, total circling $\Phi(k)$ becomes an odd times of 2π, the two-loop link must change into a knot. A topological phase with an even number of band degenerate points is represented by a two-loop link. Thus, the band degenerate induces the transition of an eigenstate graph between the link and knot.

Knot topology is characterized by using crossing number $c(K)$, which is defined as a minimal number of loop intersections in any planar representation,[1] and K in the bracket represents the knot. The transition between a link and knot, and between two different links/knots with different linking/crossing numbers are only achieved by untying two closed curves and by alternatively reconnecting the endpoints. Continuous deformation cannot change the type of knots and links. This observation indicates the robustness of the ground state provided by topological protection.

All knots represent gapless phases. Considering the gapless phase as the boundary of two gapped phases A and B, if the linking numbers of two gapped phases have an even difference and the in-between gapless phase has an even number of degenerate points, the two bands are mixed because of the band degeneracy and switch even times. The gapless phase is represented by a link with the following linking number $L = (L_\mathrm{A} + L_\mathrm{B})/2$. If the linking numbers of the two gapped phases have an odd difference and the in-between gapless phase has an odd number of degenerate points, the gapless phase is represented by a knot, and the crossing number is $c(K) = L_\mathrm{A} + L_\mathrm{B}$. In knot representation, a gapless phase with an even number of band degenerate points never has the same linking number as that of a gapped phase on either side of the gapless phase. Thus, all types of topological phases are directly distinguishable based on the knot topology of eigenstate graphs.

The linking number for links as well as the crossing number for knots relate to the number of topological protected Majorana zero modes (edge states), which are exponentially localized at the two boundaries. The results are in agreement with the prediction in a 1D noninteracting spinless fermions chain of the BDI class[57] (a topological class with time-reversal symmetry, particle-hole symmetry and chiral symmetry) with long-range coupling.[56] In the system we discussed as follows, the number of zeros multiplied their degrees minus the order of pole within the unit circle of the complex function of the effective magnetic field $B_x(k) + iB_y(k) = \sum_n J_n z^n$ defines a topological invariant that equals the number of Majorana zero modes,[56] where $z = e^{ik}$ and $J_{n>0} = (J_n^+ + J_n^-)/8$, $J_{n<0} = (J_n^+ - J_n^-)/8$, and $J_{n=0} = -g/4$ is the long range couplings; and the analysis of the complex function $B_x(k)+iB_y(k)$ is in accordance with the obtained winding number that is associated with the Bloch vector $(B_x(k), B_y(k))$ (see the Supplementary Material). In the gapped phase, the system has L pairs of Majorana zero modes. In the gapless phase, the system has $[c(K)/2]$ pairs of Majorana zero modes for the topological phase with a knot eigenstate graph, where the bands have one band-touching degeneracy points, and $[c(K)/2]$ refers to the maximal integer number that is not larger than $c(K)/2$. In the gapless phase, the system has $L - 1$ pairs of Majorana zero modes in the

topological phase with a link eigenstate graph, where the system has a two-band touching degeneracy point.

One-Dimensional XY Model. To demonstrate the rich topological features of ground states in different gapped and gapless phases, we consider a quantum spin model with the interactions (J_n^x, J_n^y) and the transverse field $g = 0$. To observe topological phases with high winding numbers, a large M is required in Hamiltonian H, and the system has long-range interactions (in the numerical analysis, we set $M = 5$). We consider the interaction between spins exponentially decay as their distances. As an example, the interactions are set as follows:

$$\begin{aligned} J_n^x &= \exp[-(2x+n-3)^2], \\ J_n^y &= 2(y-1)\exp[-(2y+n-2)^2], \end{aligned} \tag{10}$$

where x and y determine the strengths of interactions. Rich topological phases are obtained because of long-range interactions. The boundary of different phases is obtained by calculating the band gap closing condition, i.e., $\epsilon_{k_c}^{\pm} = 0$. The corresponding winding number can be obtained through a numerical integration of Eq. (6).

Alternatively, the eigenstate graph provides a clear picture and a convenient approach for identifying the topological properties of different ground states in the spin system. The topological properties of the ground states are revealed using the geometric topologies of eigenstate knots and links. The geometric topologies of knots and links only change for the untying and reconnecting of the components (loops), which are helpful for understanding topological phase transition in the quantum spin system. The eigenstate knots and links of different topological phases are shown in Fig. 1.

The gapped phase corresponds to a link, where the linking number is equal to the corresponding winding number ($L = w$). In the first row of Fig. 1, the topological phases with winding numbers $w = 1$ to 5 are elucidated through their eigenstate graphs with $L = 1$ to 5, respectively. $L = 0$ (not shown) is unknotted and corresponds to a topologically trivial phase. Moreover, with k increasing, two loops are rotated clockwise (counterclockwise) in the cross section of the torus if the linking number of the graph is positive (negative). The graph in Fig. 1 with $L = 1$ shows a Hopf link, with a winding number of $w = 1$ represented by 2_1^2. The graph with $L = 2$ presents a Solomon knot, it belongs to a link in contrast to its name and its notation is 4_1^2. The graph with $L = 3$ is the star of David denoted as 6_1^2.

The gapless phase separates two gapped phases with linking numbers $L_{\rm A}$ and $L_{\rm B}$, and its eigenstate graph corresponds to a link with a linking number of $L = (L_{\rm A} + L_{\rm B})/2$ for two degenerate points in the energy band. The graphs are similar to those in the first and third rows of Fig. 1.

The gapless phase separating the gapped phases with linking numbers $L_{\rm A}$ and $L_{\rm B}$ corresponds to a knot with a crossing number of $c(K) = L_{\rm A} + L_{\rm B}$ for one band degenerate point. With the increasing k, the point on the knot is rotated clockwise (counterclockwise) in the cross section of the torus if the crossing number of the graph is positive (negative). The second and fourth rows in Fig. 1 show knots that separate gapped phases in the first and third rows, where each knot denotes the gapless phase between the two gapped phases represented by the two nearest aforementioned links. The band-touching degeneracy point appears at $k = \pm\pi$. The gapless phase with a crossing number of $c(K) = 3$ has a positive trefoil knot, and it separates gapped phases with $L_{\rm A} = 1$ and $L_{\rm B} = 2$. The corresponding trefoil knot in the fourth row marked with 3_1 is a negative trefoil knot, and its crossing number is $c(K) = -3$. A pentafoil/cinquefoil knot with a crossing number of $c(K) = 5$ separates the gapped phases with $L_{\rm A} = 2$ and $L_{\rm B} = 3$, the $c(K) = -5$ knot is marked with 5_1. The knot with crossing number $c(K) = 7$ [$c(K) = 9$] represents the gapless phase, which separates the gapped phases with $L_{\rm A} = 3$ and $L_{\rm B} = 4$ ($L_{\rm A} = 4$ and $L_{\rm B} = 5$). The number of knot windings on the torus is $c(K)$ and has a $c(K)$ number of crossing points in a planar plane.

In summary, we have presented a graphic approach to investigate the topological phase transition in a quantum spin system. The eigenstates completely encode topological features, which are vividly revealed from the eigenstate curves, tangled and braided around each other into knots and links. The geometric topologies of knots and links represent the topological properties of different ground states, and characterize the topologies of both the gapped and gapless phases. The graphic approach highlights the interactivity of the energy bands. Our findings provide insights into applications of knot theory in quantum spin systems and topological phases of matter.

References

[1] Adams C C 1994 *The Knot Book* (New York: Freeman)
[2] Alexander J W and Briggs G B 1926 *Ann. Math.* **28** 562
[3] Wasserman S A, Dungan J M and Cozzarelli N R 1985 *Science* **229** 171
[4] Forgan R S, Sauvage J P and Stoddart J F 2011 *Chem. Rev.* **111** 5434
[5] Wilczek F and Zee A 1983 *Phys. Rev. Lett.* **51** 2250
[6] Rovelli C and Smolin L 1988 *Phys. Rev. Lett.* **61** 1155
[7] Yang C N and Ge M L 1989 *Braid Group, Knot Theory and Statistical Mechanics* (Singapore: World Scientific)
[8] Wu F Y 1992 *Rev. Mod. Phys.* **64** 1099
[9] Atiyah M 1995 *Rev. Mod. Phys.* **67** 977
[10] Katritch V, Bednar J, Michoud D, Scharein R G, Dubochet J and Stasiak A 1996 *Nature* **384** 142

[11] Faddeev L and Niemi A J 1997 *Nature* **387** 58
[12] Kauffman L H 2005 *Rep. Prog. Phys.* **68** 2829
[13] Kleckner D and Irvine W T M 2013 *Nat. Phys.* **9** 253
[14] Ren J R, Zhu T and Duan Y S 2008 *Chin. Phys. Lett.* **25** 353
[15] Kleckner D, Kauffman L H and Irvine W T M 2016 *Nat. Phys.* **12** 650
[16] Leach J, Dennis M R, Courtial J and Padgett M J 2004 *Nature* **432** 165
[17] Dennis M R, King R P, Jack B, O'Holleran K and Padgett M J 2010 *Nat. Phys.* **6** 118
[18] Taylor A J and Dennis M R 2016 *Nat. Commun.* **7** 12346
[19] Hall D S, Ray M W, Tiurev K, Ruokokoski E, Gheorghe A H and Möttönen M 2016 *Nat. Phys.* **12** 478
[20] Sun X Q, Lian B and Zhang S C 2017 *Phys. Rev. Lett.* **119** 147001
[21] Chang G, Xu S Y, Zhou X, Huang S M, Singh B, Wang B, Belopolski I, Yin J, Zhang S, Bansil A, Lin H and Hasan M Z 2017 *Phys. Rev. Lett.* **119** 156401
[22] Chen W, Lu H Z and Hou J M 2017 *Phys. Rev. B* **96** 041102(R)
[23] Ezawa M 2017 *Phys. Rev. B* **96** 041202(R)
[24] Bi R, Yan Z, Lu L and Wang Z 2017 *Phys. Rev. B* **96** 201305(R)
[25] Yan Z, Bi R, Shen H, Lu L, Zhang S C and Wang Z 2017 *Phys. Rev. B* **96** 041103(R)
[26] Chang P Y and Yee C H 2017 *Phys. Rev. B* **96** 081114(R)
[27] Ackerman P J and Smalyukh I I 2017 *Phys. Rev. X* **7** 011006
[28] Deng D L, Wang S T, Shen C and Duan L M 2013 *Phys. Rev. B* **88** 201105(R)
[29] Deng D L, Wang S T, Sun K and Duan L M 2018 *Chin. Phys. Lett.* **35** 013701
[30] Yan Q, Liu R, Yan Z, Liu B, Chen H, Wang Z and Lu L 2018 *Nat. Phys.* **14** 461
[31] Yang Z, Chiu C K, Fang C and Hu J 2020 *Phys. Rev. Lett.* **124** 186402
[32] Yuan X X, He L, Wang S T, Deng D L, Wang F, Lian W Q, Wang X, Zhang C H, Zhang H L, Chang X Y and Duan L M 2017 *Chin. Phys. Lett.* **34** 060302
[33] Yang Z and Hu J 2019 *Phys. Rev. B* **99** 081102(R)
[34] Carlström J and Bergholtz E J 2018 *Phys. Rev. A* **98** 042114
[35] Carlström J, Strälhammar M, Budich J C and Bergholtz E J 2019 *Phys. Rev. B* **99** 161115(R)
[36] Lee C H, Li G, Liu Y, Tai T, Thomale R and Zhang X 2018 arXiv:1812.02011 [cond-mat.mes-hall]
[37] Yang X M, Wu H C, Wang P, Jin L and Song Z 2020 *J. Phys. Commun.* **4** 095005
[38] Wu H C, Yang X M, Jin L and Song Z 2020 *Phys. Rev. B* **102** 161101(R)
[39] Hu H and Zhao E 2021 *Phys. Rev. Lett.* **126** 010401
[40] Feynman R P 1949 *Phys. Rev.* **76** 769
[41] Zak J 1989 *Phys. Rev. Lett.* **62** 2747
[42] Xiao D, Chang M C and Niu Q 2010 *Rev. Mod. Phys.* **82** 1959
[43] Xu S, Zhou L, Wang X Y, Wang H, Lin J F, Zeng X Y, Cheng P, Weng H and Xia T L 2020 *Chin. Phys. Lett.* **37** 107504
[44] Gong Y, Guo J, Li J, Zhu K, Liao M, Liu X, Zhang Q, Gu L, Tang L, Feng X, Zhang D, Li W, Song C, Wang L, Yu P, Chen X, Wang Y, Yao H, Duan W, Xu Y, Zhang S C, Ma X, Xue Q K and He K 2019 *Chin. Phys. Lett.* **36** 076801
[45] Jiang G, Feng Y, Wu W, Li S, Bai Y, Li Y, Zhang Q, Gu L, Feng X, Zhang D, Song C, Wang L, Li W, Ma X C, Xue Q K, Wang Y and He K 2018 *Chin. Phys. Lett.* **35** 076802
[46] Chen C, Liu Q, Zhang T Z, Li D, Shen P P, Dong X L, Zhao Z X, Zhang T and Feng D L 2019 *Chin. Phys. Lett.* **36** 057403
[47] Pei C, Xia Y, Wu J, Zhao Y, Gao L, Ying T, Gao B, Li N, Yang W, Zhang D, Gou H, Chen Y, Hosono H, Li G and Qi Y 2020 *Chin. Phys. Lett.* **37** 066401
[48] Deng H X, Song Z G, Li S S, Wei S H and Luo J W 2018 *Chin. Phys. Lett.* **35** 057301
[49] Zhang G, Li C and Song Z 2017 *Sci. Rep.* **7** 8176
[50] Suzuki M 1971 *Prog. Theor. Phys.* **46** 1337
[51] Perk J H H 2017 arXiv:1710.03384 [cond-mat.stat-mech]
[52] Sachdev S 1999 *Quantum Phase Transitions* (Cambridge: Cambridge University Press)
[53] Kitaev A Y 2001 *Phys. Usp.* **44** 131
[54] Niu Y, Chung S B, Hsu C H, Mandal I, Raghu S and Chakravarty S 2012 *Phys. Rev. B* **85** 035110
[55] Alexander J W 1923 *Trans. Am. Math. Soc.* **20** 275
[56] Verresen R, Jones N G and Pollmann F 2018 *Phys. Rev. Lett.* **120** 057001
[57] Ryu S, Schnyder A P, Furusaki A and Ludwig A W W 2010 *New J. Phys.* **12** 065010

SUPPLEMENTARY MATERIAL FOR "KNOT TOPOLOGY IN QUANTUM SPIN SYSTEM"

X. M. Yang, L. Jin, and Z. Song
School of Physics, Nankai University, Tianjin 300071, China

A: Bloch vector and winding number

The planar Bloch vector in the plane B_x-B_y for the situations shown in Fig. 1 of the main text is depicted in Fig. S1. The winding of Bloch vector around the origin (black dot) of B_x-B_y plane in the gapped phase is w. The arrows indicate the direction of the curves as k increasing from 0 to 2π; the counterclockwise (clockwise) direction yields the $+$ $(-)$ sign of the winding number. In the first and third rows, the curve of Bloch vector encloses the origin one to five times from the left to right, and the winding number in Eq. (6) of the main text is $w = \pm 1$ to $w = \pm 5$, respectively. In the second and fourth rows, the curve of Bloch vector passes through the origin. Thus, the winding number of the effective planar magnetic field is not well-defined in the gapless phase.

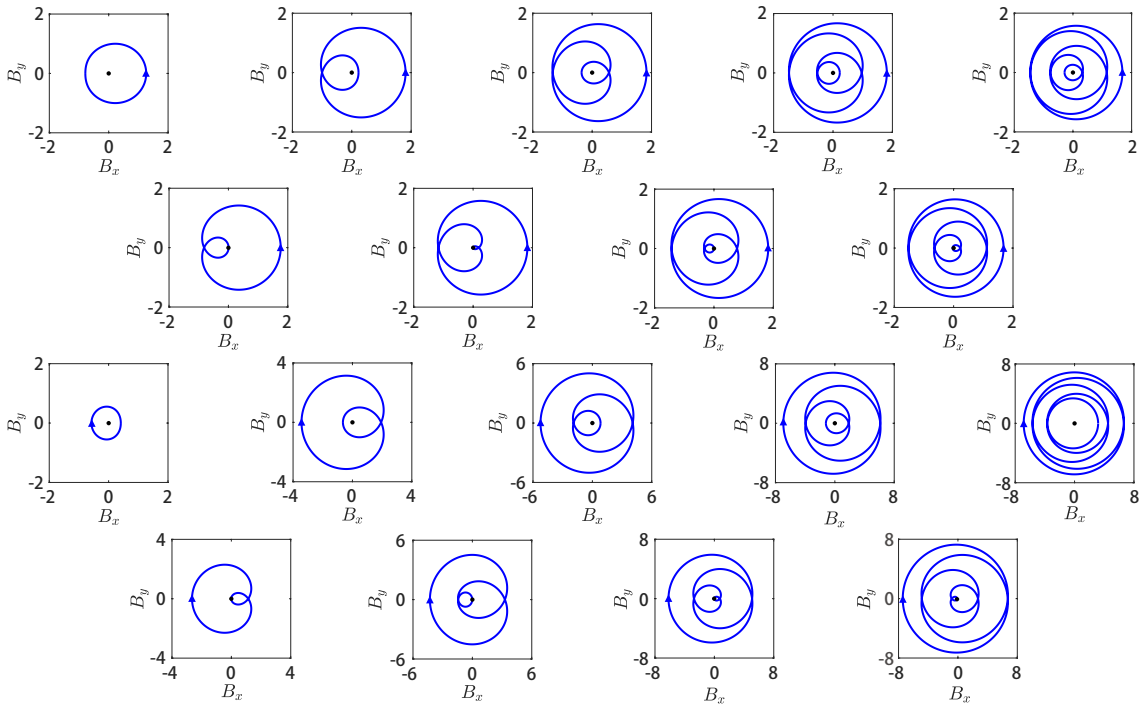

FIG. S1. Curve of Bloch vector in the B_x-B_y plane, the black dot is the origin. The corresponding knot or link eigenstate graph is depicted in Fig. 1 of the main text.

B: Linking number

In the gapped phase, the eigenstates $\left|\psi_k^{\pm}\right\rangle$ are represented by two loops on a torus surface, forming a torus link [Fig. S2(a)]. $\mathbf{r}_+(k)$ (blue loop) and $\mathbf{r}_-(k')$ (red loop) represent the positive branch $\left|\psi_k^{+}\right\rangle$ and the negative branch $\left|\psi_{k'}^{-}\right\rangle$, respectively. We construct a vector field

$$\mathbf{h}(k,k') = \mathbf{r}_+(k) - \mathbf{r}_-(k'), \tag{1}$$

where $\mathbf{r}_+(k)$ and $\mathbf{r}_-(k')$ in the cylindrical coordinate [Fig. S2(b)] are expressed as

$$\begin{aligned}\mathbf{r}_+(k) &= 0\hat{\boldsymbol{\theta}} + r\sin\varphi_+(k)\,\hat{\mathbf{z}} + [R + r\cos\varphi_+(k)]\,\hat{\mathbf{r}},\\ \mathbf{r}_-(k') &= 0\hat{\boldsymbol{\theta}}' + r\sin\varphi_-(k')\,\hat{\mathbf{z}}' + [R + r\cos\varphi_-(k')]\,\hat{\mathbf{r}}'.\end{aligned} \tag{2}$$

On the torus, R (in red) is the distance from the center of the tube to the center of the torus, and r (in purple) is the radius of the tube. Two cylindrical coordinates are related as follows

$$\hat{\mathbf{z}}' = \hat{\mathbf{z}}, \hat{\mathbf{r}}' = \cos(k'-k)\,\hat{\mathbf{r}} + \sin(k'-k)\,\hat{\boldsymbol{\theta}}. \tag{3}$$

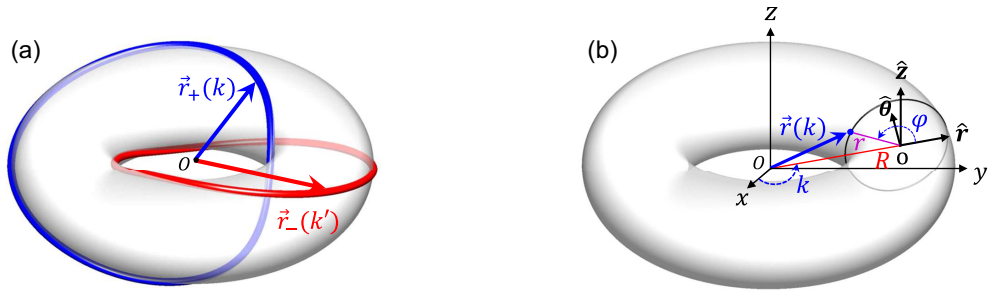

FIG. S2. (a) A two-component Hopf link lies on the torus surface, each component is a closed loop of the eigenstate $|\psi_k^{\pm}\rangle$. (b) The cylindrical coordinate for the torus.

Besides, we have $\varphi_-(k) = \varphi_+(k) + \pi$ and $\varphi_-(k') = \varphi_+(k') + \pi$. Based on these relations, we have

$$\mathbf{h}(k, k') = h_\theta \hat{\boldsymbol{\theta}} + h_z \hat{\mathbf{z}} + h_r \hat{\mathbf{r}}, \tag{4}$$

where

$$\begin{aligned} h_\theta &= [R - r\cos\varphi_+(k')]\sin(k - k'), \\ h_z &= r\sin\varphi_+(k) + r\sin\varphi_+(k'), \\ h_r &= R + r\cos\varphi_+(k) - [R - r\cos\varphi_+(k')]\cos(k - k'). \end{aligned} \tag{5}$$

Each point (k, k') is mapped to a three-dimensional vector $\mathbf{h}$. Since k and k' are periodic parameters, the endpoint of vector $\mathbf{h}$ draws a deformed torus surface in the $(\boldsymbol{\theta}, \mathbf{z}, \mathbf{r})$ space.

After introducing the vector field $\mathbf{h}$, we note that the linking number of two curves $\mathbf{r}_+(k)$ and $\mathbf{r}_-(k')$ in Eq. (8) of the main text can be expressed in the form of

$$L = \frac{1}{4\pi}\oint_k \oint_{k'} \frac{\mathbf{h}}{|\mathbf{h}|^3} \cdot \left(\frac{\partial \mathbf{h}}{\partial k}\mathrm{d}k \times \frac{\partial \mathbf{h}}{\partial k'}\mathrm{d}k'\right). \tag{6}$$

Mathematically, the above expression of linking number is equal to the solid angle subtended by the deformed torus surface divided by 4π [1]. Since the deformed torus is irregularly shaped and solid angle is hard to be calculated, we choose a cross section that contains the origin $(0, 0, 0)$ in the $(\boldsymbol{\theta}, \mathbf{z}, \mathbf{r})$ space, whose plane angle of the curve in the cross section of the deformed torus surface is half the solid angle. By doing this, we can easily get the solid angle of the deformed torus and then obtain corresponding linking number.

To get the cross section containing the origin, we set $h_\theta = 0$. The $h_\theta = 0$ plane cuts off the deformed torus surface to a curve in the $(\mathbf{z}, \mathbf{r})$ plane. By setting $h_\theta = 0$, we have $k' = k$ and $\mathbf{h}$ is reduced to

$$\mathbf{h} = h_z \hat{\mathbf{z}} + h_r \hat{\mathbf{r}} = 2r\sin\varphi_+(k)\,\hat{\mathbf{z}} + 2r\cos\varphi_+(k)\,\hat{\mathbf{r}}, \tag{7}$$

which indicates a closed circle Γ centered at $(0, 0)$ in the $(\mathbf{z}, \mathbf{r})$ plane and the linking number defined by the vector field $\mathbf{h}$ is given by

$$\begin{aligned} L &= \frac{1}{2\pi}\oint_\Gamma \frac{1}{4r^2}(h_z \nabla_k h_r - h_r \nabla_k h_z)\mathrm{d}k \\ &= -\frac{1}{2\pi}\int_0^{2\pi} \nabla_k \varphi_+(k)\,\mathrm{d}k. \end{aligned} \tag{8}$$

Furthermore, from the definition $\varphi_+(k) = \arctan(-B_y/B_x)$, the linking number Eq. (8) can be expressed as

$$L = \frac{1}{2\pi}\oint_C \frac{1}{B^2}(B_x \mathrm{d}B_y - B_y \mathrm{d}B_x) = w. \tag{9}$$

The linking number L is equivalent to the winding number w defined in Eq. (6) of the main text.

[1] J. K. Asbóth, L. Oroszlány, and A. Pályi, *A Short Course on Topological Insulators: Band-structure topology and edge states in one and two dimensions* (Springer, 2016).